EXTENDING STABLE OPERATION RANGE IN HALL THRUSTERS

38th AIAA/ASME/SAE/ASEE Joint Propulsion Conference & Exhibit
7-10 July 2002, Indianapolis, Indiana
AIAA 2002-3953

Naoji Yamamoto* Takafumi Nakagawa†, Kimiya Komurasaki‡ and Yoshihiro Arakawa§
University of Tokyo, Hongo 7-3-1, Bunkyo-ku, Tokyo, 113-8656, Japan

Abstract

Characteristics of discharge oscillations at a frequency range of 10-100kHz in a Hall thruster were investigated using a 1kW class anode layer type Hall thruster. An oscillation model was proposed where the oscillation is due to ionization interaction between electrons and neutral particles and where the phase velocity of electrons is different from that of neutral particles. The predicted unstable operational condition agreed with the experimental results in tendency. This model shows that decrease in cross section of discharge chamber should make stable operation range extended, and experimental results supported this assumption.

Nomenclature

A	:	oscillation amplitude
B	:	magnetic flux density
D	:	diffusion coefficient
E	:	electric field strength
e	:	electronic charge
I_d	:	discharge current
I_{sp}	:	specific impulse
k	:	wave number
k_B	:	Boltzmann's constant
L	:	ionization zone length
M	:	particle mass
$\dot{m}$	:	mass flow rate
N	:	number density
P	:	pressure
Q	:	particle flow rate
r_L	:	Larmor radius
S	:	cross-section
T	:	temperature
V	:	volume
V_e	:	electron velocity
V_n	:	neutral atom velocity
V_d	:	discharge voltage
z	:	axial direction
α	:	ion loss coefficient
β	:	excitation coefficient
γ	:	ionization coefficient
ε	:	ionization energy
η_u	:	propellant utilization
λ_{ne}	:	neutral-electron mean free path
μ	:	mobility
τ	:	measurement time
ϕ	:	space potential
ω	:	oscillation frequency

Subscripts

e	:	electron
i	:	ion
n	:	neutral atom
w	:	wall
anode	:	anode side
exit	:	exit side

Introduction

A Hall thruster is one of the promising thrusters for satellite station keeping and orbit transfer, since it has an attractive combination of high thrust efficiency with specific impulse of 1000-3000sec, high thrust efficiency of more than 50% and high thrust-to-power ratio as compared to an ion thruster. Therefore, there will be many missions using a Hall thruster.[1)] There, however, are still some challenges for practical application. One of these challenges is the suppression of plasma oscillations. Plasma oscillations cause the operation to cease as well as they bear down on PPU. Especially oscillations at a frequency range of 10-100kHz are the largest oscillations of all and often cause the discharge to cease. There have been many studies about these oscillation phenomena, and they revealed that these oscillations would be caused by ionization instability.[2-4)] They, however, were not enough to adequately describe this oscillation, especially stability criteria for a certain range of magnetic flux density or mass flow rate. The aim of this study is 1) to investigate the characteristics of the oscillation, 2) to propose a physical model and 3) to propose the way to depress the oscillation.

*Graduate student, Department of Aeronautics and Astronautics, student member AIAA
†Graduate student, Department of Aeronautics and Astronautics
‡Associate Professor, Department of Advanced Energy, Member AIAA
§Professor, Department of Aeronautics and Astronautics, Member AIAA

The Experimental Equipment

Thruster

Figure 1 shows the cross-section of a 1kW class anode layer type Hall thruster. It has two guard rings made of stainless steel. They are kept at cathode potential. The inner and outer diameter of the discharge chamber is 48mm and 72mm, respectively. The outer diameter can be changed to 62mm. It has a hollow annular anode. The anode is located at 3mm upstream end of the discharge chamber. A solenoidal coil is set at the center of the thruster to apply radial magnetic field in the discharge chamber. The magnetic flux density is variable by changing the coil current. Figure 2 shows the magnetic field distribution along the chamber median at the coil current of 4A. Magnetic flux density is maximum at the chamber exit and minimum at the anode.

Xenon was used as a propellant gas. As an electron source, a filament cathode (ϕ 0.27mm×500mm×3, 2% thoriated tungsten) was used, since the hollow cathode in itself can be a noise source as shown in Fig. 3.

Vacuum Chamber

A 2m-diameter by 3m long vacuum chamber was used through the experiments. The pumping system consists of a diffusion pump, a mechanical booster pump and two rotary pumps. These pumps give the facility an air-pumping speed of 30,000l/s and the ultimate base pressure is 4.5×10^{-4} Pa. The background pressure was maintained at less than 5.3×10^{-3} Pa when the Hall thruster was operating with 3.4mg/s of xenon.

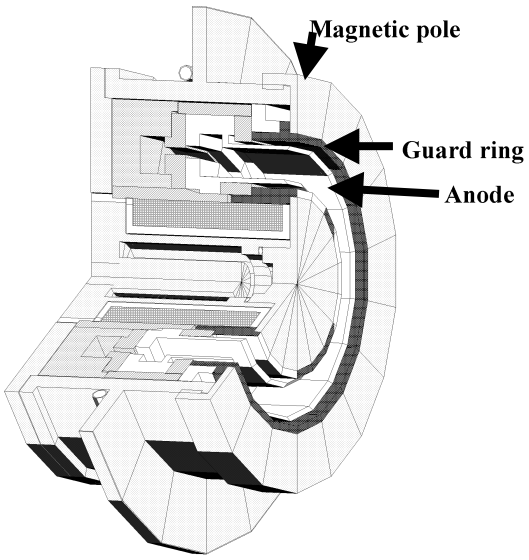

Fig. 1 Cross section of the anode layer type Hall Thruster developed at University of Tokyo.

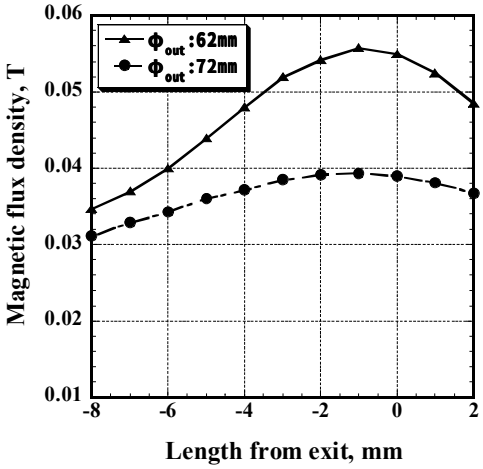

Fig. 2 Magnetic flux density profile.

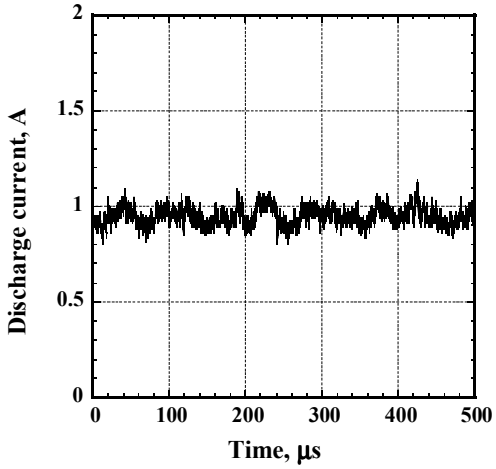

Fig. 3 Discharge current trace of a hollow cathode.

Results and Discussion

Oscillation Characteristics

To examine experimental results, the amplitude of oscillation is defined as,

$$A = \frac{R.M.S}{\overline{I_d}} = \frac{1}{\overline{I_d}}\sqrt{\frac{\int_0^\tau (I_d - \overline{I_d})^2}{\tau}}, \quad (\overline{I_d} = \frac{\int_0^\tau I_d}{\tau}) \qquad (1)$$

Figure 4 shows the effect of magnetic flux density on oscillation characteristics. The oscillation characteristics were changed sensitively with *B*. They can be categorized into four regimes. The feature of each regime was shown in Ref. 5.

These results would show that the electron mobility might affect this oscillations rather than the ion mobility. Since oscillation characteristics depend on magnetic flux density as well as on discharge voltage and they were changed sensitively with the magnetic flux density.

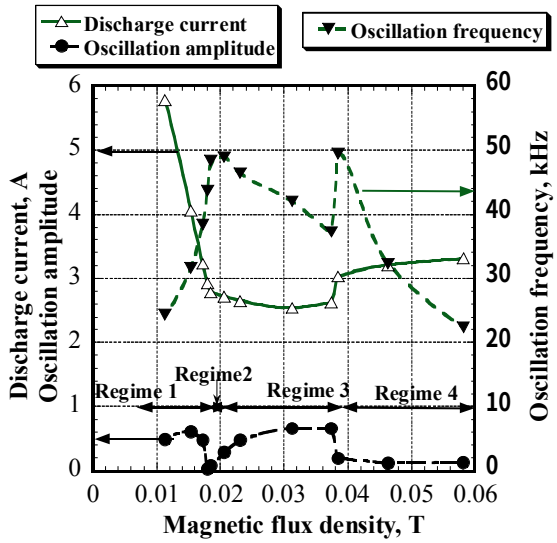

Fig. 4 Oscillation characteristics.
$\dot{m}$ =2.72mg/s, V_d=250V

Oscillation Model

Several studies indicated that the oscillation was caused by ionization instability.[2)~4)] In addition, the electron mobility is the key role on this oscillation. Considering above things, the set of equations describing the oscillation are below.

The equation of continuity for neutral atom

$$\frac{\partial N_n}{\partial t} + \nabla(N_n V_n) = -\gamma N_n N_e \qquad (2)$$

The equation of continuity for electron

$$\frac{\partial N_e}{\partial t} + \nabla(N_e V_e) = \gamma N_n V_e \qquad (3)$$

Integrating Eqs. (2) and (3) over the whole ionization zone, they can be rewritten as.

$$\begin{aligned} \int_V \frac{\partial N_n}{\partial t} dV + \int_S N_n V_n dS &= \int_V -\gamma N_n N_e dV \\ \int_V \frac{\partial N_e}{\partial t} dV + \int_S N_e V_e dS &= \int_V \gamma N_n N_e dV \end{aligned} \qquad (4)$$

These equations were solved analytically. Each parameter is assumed to consist of a steady state part and a small disturbance part that is proportional to $\exp[-i(\omega t - k z)]$. The wave number k of neutral atoms is assumed different from that of electrons, though Baranov et al. assumed that they are the same.[2)] Phase velocity in each particles is assumed as their respective axial velocity. L is no more than 0.005m and electron velocity would be more than 3000m/s, wave number of electrons was considered to vanish. Therefore, the wave number k is assumed as

$$\begin{aligned} k_n &= C_n + i\,1/\lambda_{ne} \\ k_e &= C_e + i\,1/\lambda_{en} \approx 0 \\ \text{where,}\quad C_n &\approx \mathrm{Re}[\omega]/V_n \end{aligned} \qquad (5)$$

An electron velocity is also assumed to oscillate, since electrons are thought to move to anode with classical diffusion.[5)] The electron velocity is written as

$$\begin{aligned} V_e &= -\mu_\perp E - D_\perp \frac{\nabla N_e}{N_e} = -\mu\left(E + \frac{kT_e}{e}\frac{\nabla N_e}{N_e}\right) \\ &= -\frac{m_e N_n <\sigma v>_{en}}{eB^2}\left(E + \frac{kT_e}{e}\frac{\nabla N_e}{N_e}\right) \end{aligned} \qquad (6)$$

Thus, each parameter is rewritten as below

$$\begin{aligned} N_e &= N_e + n_e \exp[-i(\omega t + k_e z)] \\ &\approx N_e + n_e \exp[-i\omega t] \\ N_n &= N_n + n_n \exp[-i(\omega t - k_n z)] \\ V_e &= V_e + v_e \\ &= -\frac{m_e <\sigma v>_{en}}{eB^2}\left(E + \frac{kT_e}{e}\frac{\nabla N_e}{N_e}\right)(N_n + n_n) \\ &\equiv f(z)(N_n + n_n) \end{aligned} \qquad (7)$$

For simplicity, an ionization zone is considered as a homogeneous box region where ionization rates, neutral atom density, and plasma density are homogeneous as shown in Fig.5. In addition, electrons don't collide with the Chamber wall and ions.

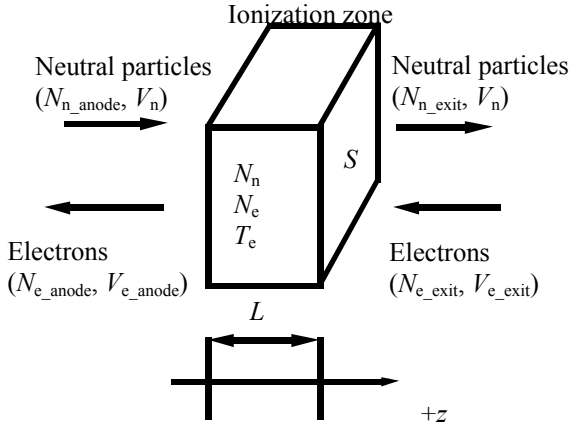

Fig.5 Schematic of ionization zone.

Substituting Eq. (5) into Eq. (4), the dispersion relation is written as,

$$\begin{aligned} &\omega^2 + \left\{ i\gamma(N_e - N_n) + i\frac{V_{e\_exit} - r_S V_{e\_anode}}{L} - GV_n \right\}\omega \\ &+ iG\left(\gamma N_n V_n - \frac{V_{e\_exit} - r_S V_{e\_anode}}{L} V_n + \gamma N_n f_{exit} N_{e\_exit} \right) \\ &- \gamma N_e \frac{V_{e\_exit} - r_S V_{e\_anode}}{L} = 0 \end{aligned} \qquad (8)$$

$$\text{where}\quad G = \frac{k_n \times \exp[ik_n L]}{\exp[ik_n L] - 1}, \qquad r_S = \frac{S_{anode}}{S_{exit}}$$

The stability condition of this oscillation Im [ω]<0 is written as,

$$b > 0 \tag{9}$$

$$b^2 c - abd + d^2 < 0 \tag{10}$$

where

$$a = -\mathrm{Re}[G] \times V_n$$

$$b = \frac{V_{e\_exit} - r_S V_{e\_anode}}{L} + \gamma (N_e - N_n) - \mathrm{Im}[G] \times V_n$$

$$c = -\mathrm{Im}[G] \times \left(\begin{array}{l} \gamma N_n V_n - \dfrac{V_{e\_exit} - r_S V_{e\_anode}}{L} V_n \\ + \gamma N_n f_{exit} N_{e\_exit} \end{array} \right) - \gamma N_e \frac{V_{e\_exit} - r_S V_{e\_anode}}{L}$$

$$d = \mathrm{Re}[G] \times \left(\begin{array}{l} \gamma N_n V_n - \dfrac{V_{e\_exit} - r_S V_{e\_anode}}{L} V_n \\ + \gamma N_n f_{exit} N_{e\_exit} \end{array} \right)$$

Equations (9) and (10) need to be rewritten about operation parameter to compare this model with the experimental results.

Neutral particles temperature is estimated as 700K, therefore the neutral atom velocity is constant as

$$V_n = \frac{1}{4} \sqrt{\frac{8 k_b T}{\pi M}} = 84 m/s \tag{11}$$

We estimate electron temperature from the electron energy balance equation as shown below.

$$\frac{5}{2} \nabla (k T_e n_e v_e) = e \Gamma_e \frac{d\phi}{dz} - (1+\beta) \gamma n_n n_e \varepsilon \tag{12}$$

The heat loss into the wall is neglected. Since the discharge chamber wall is kept at cathode potential, only ions collide with the wall chamber. Ionization potential is 12.13eV for Xenon, and the excitation coefficient is chosen as 2.0 according to Ref. 6.

According to Ref. 7, the length of ionization zone of an anode layer type is estimated as several times electron Larmor radius. Thus, it was assumed as two times electron Larmor radius unless it is beyond discharge chamber length 0.004m as shown in Fig.6. r_s is estimated as 1.1.

$$L = \begin{cases} \alpha \, \mathrm{r_{Le}} = \dfrac{2}{B} \sqrt{\dfrac{8 m_e k_B T_e}{\pi \, e}} & < 0.004 \\ 0.004 \end{cases} \tag{13}$$

The electron density is estimated as below

$$\begin{cases} N_e \approx N_i = 1.5 \times \eta_u \dfrac{\dot{m}}{M S V_{i\_exit}} \\ \eta_u = 1 - Exp(-\dfrac{0.8 \times L \gamma N_e}{V_n}) \end{cases} \tag{14}$$

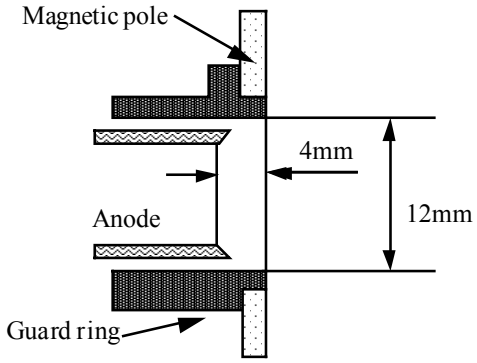

Fig.6 Schematic of discharge chamber

Figure 7 shows the measured oscillation amplitude and stable/unstable operation condition deduced from theory. The doted area indicates operational condition with no oscillation deduced from this theory. The stable operation zone deduced from this theory agreed with the experimental results in tendency. Figure 8 shows the measured oscillation frequency and the theoretical frequency. The order of deduced one agreed with that of the measured one. The difference might be due to the approximation that distribution of plasma parameters is homogenous over ionization zone. However, this model would be a good expression of this oscillation mechanism.

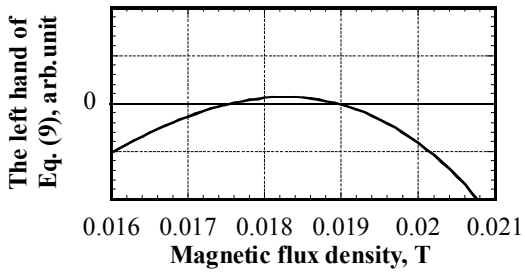

(a)

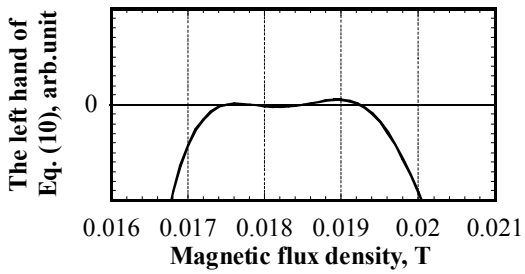

(b)

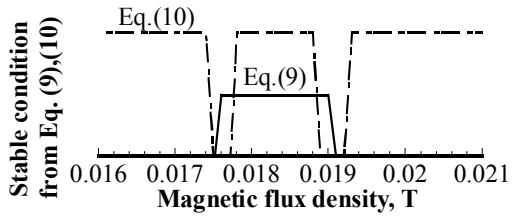

(c)

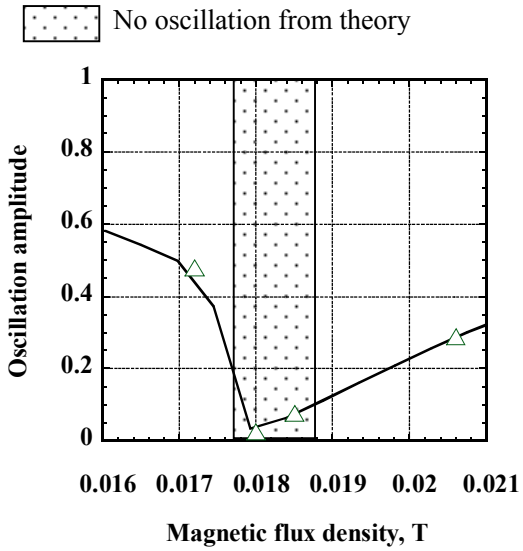

(d)

Fig. 7 Stable/unstable operational condition.
(a) Eq. (9), (b) Eq. (10), (c) Eqs. (9) and (10)
(d) Experiment $\dot{m}$=2.72mg/s, V_d=250V

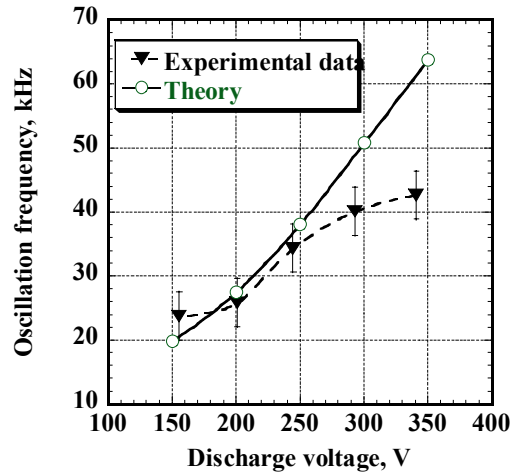

Fig. 8 Relation between frequency and discharge voltage. $\dot{m}$=2.04mg/s, B=0.02T

Examining this model, the criteria of Eq. (10) are almost covered that of Eq. (9). Therefore the criteria from equations (9) was examined.

Due to this model, decrease in cross section of discharge chamber makes operation stable. Since the left hand of equation (9) can be rewritten as

$$b = \frac{-|f_{exit}|N_{n\_exit} + r_s|f_{anode}|N_{n\_anode}}{L} + \gamma(N_e - N_n) - \mathrm{Im}[G]\times V_n$$

$$\approx \frac{-|f_{exit}|(1-\eta_u)N_{n\_anode} + r_s|f_{anode}|N_{n\_anode}}{L} + \gamma\left(\frac{N_e}{N_{e\_exit}}\eta_u N_{n\_anode} - \frac{2-\eta_u}{2}N_{n\_anode}\right)$$

$$= \frac{\dot{m}}{MSV_n}\times\left(\eta_u \times\left\{\gamma\left(\frac{N_e}{N_{e\_exit}}+\frac{1}{2}\right)+\frac{|f_{exit}|}{L}\right\} + \frac{r_s|f_{anode}|}{L} - \left(\frac{|f_{exit}|}{L}+\gamma\right)\right)$$

$$\approx \left(\left(1-Exp(-C_1\frac{\dot{m}}{S})\right)\times\left\{\gamma\left(\frac{N_e}{N_{e\_exit}}+\frac{1}{2}\right)+\frac{|f_{exit}|}{L}\right\} + \frac{r_s|f_{anode}|}{L} - \left(\frac{|f_{exit}|}{L}+\gamma\right)\right) \times\frac{\dot{m}}{MSV_n} \quad (15)$$

C_1: positive constant

To confirm this, discharge chamber was changed to a small one (outer diameter: 62mm). Figure 9 shows the results using the small chamber. The operation range of B with no oscillation was extended as shown in the theory: that is, the range of tolerant B was almost 0.01T at small chamber, though that at large chamber was about 0.001T.

This theory also shows that increase in mass flow rate extends the operation range with no oscillation. Figure 10 shows operating condition map using the small discharge chamber. Triangle shows the operational condition that A is more than 0.1. The operation range with no oscillation was extended with increase in mass flow rate. Discharge, however, became out of control when $\dot{m}$ was 4.08mg/s in this chamber configuration, that is, too much discharge current occurred and the thrust efficiency was decreased. Thus, there are optimum discharge chamber configuration if $\dot{m}$ and V_d was given.

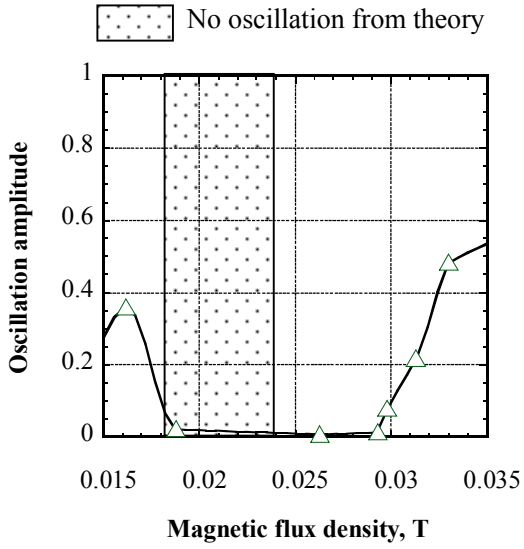

Fig. 9 Oscillation amplitude
$\dot{m}$=2.72mg/s, V_d=250V

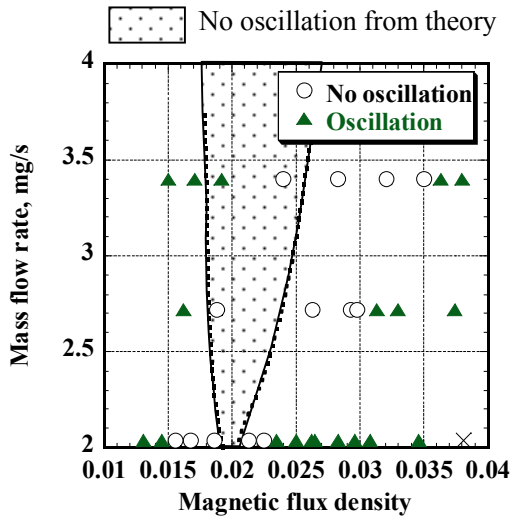

Fig. 10 Operational condition map.
V_d=250V

Summary

An ionization oscillation model considering electron dynamics was suggested. The deduced unstable operational condition agreed qualitatively with the experimental results. This model proposed that increasing mass flow rate should make the operation stable, and experimental results supported this assumption.

References

[1] Saccoccia.G "European Activity in Electric Propulsion" IEPC-01-006, 27th International Electric Propulsion Conference, Pasadena, CA, October 2001.

[2] Baranov V. I., Nazarenko Yu. S., Petrosov V. A., Vasin A. I., and Yashonov Yu. M. "Theory of oscillations and Conductivity For Hall Thruster" AIAA 96-3192, 32nd AIAA/ASME/SAE/ASEE joint Propulsion Conference, Lake Buena Vista, FL, July 1996

[3] Fife, J. M., Martinez-Sanchez, Manuel, and Azabo, James "A numerical study of low-frequency discharge oscillations in Hall thrusters" AIAA96-3052, 33rd AIAA/ASME/SAE/ASEE joint Propulsion Conference. Seattle, WA, July, 1997

[4] Darnon F., Kadlec-Philippe C., Bouchoule A., and Lyszuk M. "Dynamic Plasma & Plume Behavior of SPT thrusters" AIAA98-3644, 34th AIAA/ASME/SAE/ASEE joint Propulsion Conference. July 1998, Cleveland, OH

[5] Yamamoto N., Nakagawa T., Komurasaki K. and Arakawa Y. "Discharge plasma Fluctuations in Hall Thrusters" Vacuum, vol.65, issues 3-4, 2002, pp. 375-381

[6] Smirnov V. A., "Electron Energy Balance in a Hall-Current Accelerator with an Extended Acceleration zone" Soviet Journal of Plasma Physics, Vol. 5, No.2,1979, pp.202-205.

[7] Popov Yu. S. and Zolotaikin Yu M. "Effect of Anomalous Conductivity on the Structure of the anode Sheath in a Hall Current ion source" Sov. J. Plasma Phys., Vol. 3, No.2 March-April 1977 pp. 210-213